

- (2) H. Oberhammer and W. Zeil, to be submitted for publication.
- (3) G. Herzberg, "Molecular Spectra and Molecular Structure", Vol. II, Van Nostrand, Princeton, N.J., 1945.
- (4) E. B. Wilson Jr., J. C. Decius, and P. C. Cross, "Molecular Vibrations", McGraw-Hill, New York, 1955.
- (5) H. Siebert, "Anwendungen der Schwingungsspektroskopie in der Anorganischen Chemie", Springer Verlag, Heidelberg, 1966.
- (6) T. Ueda and T. Shimanouchi, *J. Mol. Spectrosc.*, **28**, 350 (1968).
- (7) R. Steudel, *Z. Anorg. Allg. Chem.*, **361**, 180 (1968).
- (8) L. H. Jones, "Inorganic Vibrational Spectroscopy", Marcel Dekker, New York, 1971.
- (9) A. Haas, H. Willner, H. Burger, and G. Pawelke, *Spectrochim. Acta, Part A*, **33a**, 937 (1977).
- (10) M. J. Hopper, J. W. Russel, and J. Overend, *Spectrochim. Acta, Part A*, **28a**, 1215 (1972).
- (11) J. H. Carpenter, D. F. Rimmer, J. G. Smith, and D. H. Whiffen, *J. Chem. Soc., Faraday Trans. 2*, **71**, 1752 (1975).
- (12) G. B. Aitken, J. L. Duncan, and G. P. McQuillan, *J. Chem. Soc. A*, 2695 (1971).
- (13) D. W. Scott, *J. Mol. Spectrosc.*, **31**, 451 (1969).
- (14) W. D. Horrocks and F. A. Cotton, *Spectrochim. Acta*, **17**, 134 (1961).
- (15) T. M. Barakat, N. Legge, and A. D. E. Pullin, *Trans. Faraday Soc.*, **59**, 1733, 1764 (1963).
- (16) D. M. Yost, C. C. Steffens, and S. T. Gross, *J. Chem. Phys.*, **2**, 311 (1934).
- (17) V. D. Klimov and E. A. Lobikov, *Opt. Spectrosc. (USSR)*, **30**, 25 (1971).
- (18) R. S. McDowell, J. P. Aldridge, and R. F. Holland, *J. Phys. Chem.*, **80**, 1203 (1976).
- (19) W. V. F. Brooks, M. Eshaque, C. Lau, and J. Passmore, *Can. J. Chem.*, **54**, 817 (1976).
- (20) K. O. Christe, E. C. Curtis, C. J. Schack, S. J. Cyvin, J. Brunvoll, and W. Sawodny, *Spectrochim. Acta, Part A*, **32a**, 1141 (1976).
- (21) K. O. Christe, C. J. Schack, and E. C. Curtis, *Inorg. Chem.*, **11**, 583 (1972).
- (22) K. O. Christe, E. C. Curtis, C. J. Schack, and A. Roland, *Spectrochim. Acta, Part A*, **33a**, 69 (1977).
- (23) K. O. Christe, C. J. Schack, D. Pilipovich, E. C. Curtis, and W. Sawodny, *Inorg. Chem.*, **12**, 620 (1973).
- (24) K. O. Christe, E. C. Curtis, C. J. Schack, and D. Pilipovich, *Inorg. Chem.*, **11**, 1679 (1972).
- (25) K. Sathianadan, K. Ramaswamy, S. Sundaram, and F. F. Cleveland, *J. Mol. Spectrosc.*, **13**, 214 (1964).
- (26) I. W. Levin, *J. Chem. Phys.*, **55**, 5393 (1971).
- (27) K. O. Christe and W. Sawodny, *J. Chem. Phys.*, **52**, 6320 (1970).
- (28) A. Haas and H. Willner, *Spectrochim. Acta, Part A*, **34a**, 541 (1978).
- (29) D. C. McKean, J. L. Duncan, and L. Batt, *Spectrochim. Acta, Part A*, **29a**, 1037 (1973).
- (30) D. C. McKean, *Spectrochim. Acta, Part A*, **31a**, 1167 (1975).
- (31) J. H. Schachtschneider, Technical Report 231-64, Project 31450, Shell Development Co., Emeryville, Calif., 1964.
- (32) S. Sunder, Ph.D. Thesis, University of Alberta, Edmonton, Alberta, Canada, 1972.
- (33) J. H. Schachtschneider, Technical Report 57-65, Project 31450, Shell Development Co., Emeryville, Calif., 1964.
- (34) R. S. Berry, *J. Chem. Phys.*, **32**, 933 (1960).
- (35) R. S. Berry, *Rev. Mod. Phys.*, **32**, 447 (1960).
- (36) I. W. Levin and W. C. Harris, *J. Chem. Phys.*, **55**, 3048 (1971).
- (37) Reference 3, p 232.
- (38) Reference 5, p 36.

Contribution from the Department of Chemistry, University of New Hampshire, Durham, New Hampshire 03824, the Department of Chemistry and Biochemistry, Utah State University, Logan, Utah 84322, and the Department of Chemistry, University of Arizona, Tucson, Arizona 85721

Electron Paramagnetic Resonance Structural Studies of Molybdenum(V)-Oxo Complexes

M. I. SCULLANE,^{1a} R. D. TAYLOR,^{1b} M. MINELLI,^{1b} J. T. SPENCE,^{1b} K. YAMANOUCHI,^{1c} J. H. ENEMARK,^{1c} and N. D. CHASTEEN*^{1a}

Received April 5, 1979

EPR and optical spectral data are reported for $(\text{NH}_4)_2\text{MoOCl}_5$ and a series of its derivatives: MoOCl_3L , where L = *o*-phenanthroline and α, α' -bipyridyl; MoOCl_2 , where L = acetylacetone, 8-hydroxyquinoline, and 8-mercaptoquinoline; MoOClL , where L = disalicylaldehyde *o*-phenylenediamine, *N, N'*-dimethyl-*N, N'*-bis(2-mercaptoethyl)ethylenediamine, and *N, N'*-bis(2-methyl-2-mercaptoethyl)ethylenediamine; $\text{Et}_4\text{NMoOCl}_2\text{L}$, where L = salicylaldehyde *o*-hydroxyanil. EPR measurements were made at both X (9.5 GHz) and Q (35 GHz) band frequencies. Several of the compounds have noncoincident *g* and nuclear hyperfine tensors which aid in assigning geometrical isomers in dimethylformamide solutions. The results are discussed in terms of the molecular and electronic structures of the above compounds and their relationship to the Mo center in xanthine oxidase. The spin-orbit coupling of chloride ligands does not appear to be the dominant mechanism contributing to the *g* shift.

Introduction

The active sites of molybdenum enzymes have been investigated by using EPR to detect the Mo(V) (d^1) species present during the catalytic cycles of these enzymes.²⁻⁵ In order to obtain structural information about the molybdenum sites from EPR spectroscopy, we need data for a variety of well-characterized Mo(V) compounds. Some preliminary work in this area has been done recently on several monomeric Mo(V)-oxo complexes.^{2,6,7} We now report the results of a more detailed EPR study of a series of ten such complexes.

As a consequence of the distribution of the naturally abundant isotopes, the EPR spectra of molybdenum(V) complexes are particularly amenable to analysis. The isotopes of even atomic mass, which comprise about 75% of the total, have no nuclear spin ($I = 0$). The intense lines observed with frozen-solution samples arise from the Zeeman term in the spin Hamiltonian for the $I = 0$ isotopes and provide a direct means of measuring the principal *g* factors. The remaining two isotopes (15.72% ⁹⁵Mo and 9.46% ⁹⁷Mo) have nuclear spins of $I = 5/2$ and nearly identical magnetogyric ratios. These isotopes produce six-line hyperfine patterns of low

intensity which are distributed symmetrically with respect to the intense $I = 0$ lines. The ability to measure the *g* factors independently from the hyperfine interaction is especially helpful in the interpretation of EPR spectra of complexes of low symmetry, which may have noncoincident *g* and nuclear hyperfine tensor axes. Knowledge of the relative orientation of the tensor axes can provide structural information in some instances.

The EPR spectra of $(\text{NH}_4)_2\text{MoOCl}_5$ and a series of its derivatives, MoOCl_3L (I, L = phen; II, L = *trans*-bpy; III, L = *cis*-bpy), MoOCl_2 (IV, L = acac; V, L = ox; VI, L = tox), MoOClL (VII, L = (sal)phen; VIII, L = $\text{C}_8\text{H}_{18}\text{N}_2\text{S}_2$; IX, L = $\text{C}_{10}\text{H}_2\text{N}_2\text{S}_2$), and $\text{Et}_4\text{NMoOCl}_2\text{L}$ (X, L = sap), were measured at both X- (9.5 GHz) and Q-band (34.5 GHz) frequencies in dimethylformamide (DMF) solutions.⁸ The magnetic properties are discussed in terms of the coordination geometry and bonding in these complexes.

Experimental Section

Synthesis. Syntheses of compounds I-III and V-X have been published previously.^{6,7,9-11} Compound IV was prepared as described here.

Table I. EPR Results

compd	probable equatorial ligands ^a	g_{xx} ^b	g_{yy} ^b	g_{zz} ^b	$A_{x'x'}$ ^c	$A_{y'y'}$ ^c	$A_{z'z'}$ ^c	g_0 ^b	A_0 ^c	α_{XY} ^d	α_{XZ} ^d
(NH ₄) ₂ MoOCl ₄	Cl ₄	1.938	1.938	1.970	34.0	34.0	74.5	1.946	46.6	0	0
I, <i>trans</i> -MoOCl ₃ (phen) ^e	N ₂ Cl ₂	1.941	1.929	1.971	30	38	71	1.947	46.6	0	25
II, <i>trans</i> -MoOCl ₃ (bpy)	N ₂ Cl ₂	1.944	1.931	1.971	29	35	73	1.948	46.0	0	35
III, <i>cis</i> -MoOCl ₃ (bpy)	NCl ₃	1.968	1.953	1.938	48	12	70	1.952	42.9	0	25
IV, <i>trans</i> -MoOCl(acac) ₂	O ₄	1.950	1.940	1.927	33.4	36.2	77.6	1.938	49.0	~0	~0
V, <i>cis</i> -MoOCl(ox) ₂	NO ₂ Cl	1.939	1.953	1.970	46.5	9.1	74.2	1.954	43.2	~25 ^f	~25 ^f
VI, <i>cis</i> -MoOCl(tox) ₂ ^g	NS ₂ Cl	1.948	1.952	2.003	19.5	35.5	59.2	1.967	37.9	10	~0
VII, <i>trans</i> -MoOCl(sal) ₂ (phen)	N ₂ O ₂	1.955	1.926	1.947	25.0	33.4	71.5	1.940	44.1	0	~0
VIII, <i>cis</i> -MoOCl(C ₁₀ H ₁₄ N ₂ S ₂) ^g	NS ₂ Cl	1.940	1.951	2.006	30	23	61	1.966	37.8	35	~5 ^g
IX, <i>cis</i> -MoOCl(C ₁₀ H ₂₂ N ₂ S ₂) ^g	NS ₂ Cl	1.943	1.958	2.011	22.5	36.0	57.5	1.969	38.0	30	~0
X, <i>cis</i> -(Et ₃ N)MoOCl ₃ (sap)	O ₂ Cl ₂	1.949	1.946	1.923	34.5	32.5	74.2	1.938	47.1	0	20

^a Equatorial to the MoO³⁺ group. ^b Errors in g nominally ± 0.001 . g_0 is the room-temperature solution value. ^c Units: 10^{-4} cm⁻¹. Errors nominally $\pm 0.5 \times 10^{-4}$ cm⁻¹ except for the A values less than 20×10^{-4} cm⁻¹ which have errors nominally $\pm 1 \times 10^{-4}$ cm⁻¹. A_0 is the room-temperature solution value. ^d Units: degrees. Errors nominally $\pm 5^\circ$. Values listed as 0° are required to be so by symmetry. Values listed as $\sim 0^\circ$ are zero within experimental error. ^e In each case *cis* or *trans* refers to coordination of a chloro ligand relative to oxo. ^f No axes are coincident for this compound. Values are estimates only. ^g Parameters for these compounds are further refined from those reported previously. See ref 7.

MoOCl(acac)₂ (IV). A 150-mL amount of dry benzene and 50 mL of acetylacetone were flushed with N₂ for 30 min. A 0.65-g sample of (NH₄)₂MoOCl₄ was added. The suspension was refluxed under N₂ for 1.5 h and filtered, and 90% of the solvent was evaporated under vacuum. The green solution was kept under vacuum in the freezer overnight. A yellow-green precipitate formed, which was filtered off, washed with ether, and dried under vacuum over P₂O₅. Anal. Calcd for MoOCl(C₁₀H₁₄O₄): C, 34.75; H, 4.08; Cl, 10.26. Found: C, 35.58; H, 4.19; Cl, 9.13.

Materials. (NH₄)₂MoOCl₄ was prepared and purified as previously described.¹² Tetraethylammonium chloride was obtained from Eastman.

EPR Spectra Measurements. Solutions of the various complexes were prepared to approximately 2×10^{-3} M in spectral grade DMF under dried nitrogen gas. The DMF was previously dried over molecular sieves (Fisher, Type 3A) and deoxygenated by flushing with dry N₂(g). Samples were transferred by using Becton-Dickinson disposable syringes to nitrogen-flushed, serum-stoppered EPR tubes. It was necessary to add a small amount of dry tetraethylammonium chloride (Et₄NCl) to the solutions of compounds III and VII to obtain EPR spectra of a single species.

X-Band EPR spectra were obtained on a Varian E-4 spectrometer at room temperature (~ 9.5 GHz) and 77 K (~ 9.2 GHz) with a field modulation of 100 kHz. The magnetic field was calibrated with a Newport Instruments proton NMR gaussmeter and the frequency calculated from the resonance of DPPH (diphenylpicrylhydrazyl) radical, $g = 2.0036$. Spectra were also measured at Q-band frequency (~ 35 GHz) at 110 K on a Varian E-9 spectrometer equipped with an E110 microwave bridge and high-field pole caps.

Analysis of EPR Spectra. The frozen-solution EPR spectra were simulated with a program developed by White and Belford¹³ and modified by White, Albanese, and Chasteen.^{14a} Computations were performed on a DEC-1090 computer equipped with a Calcomp plotter. Spectra were fitted with the rhombic $S = 1/2$ spin Hamiltonian

$$\mathcal{H} = \beta \vec{H} \cdot \vec{g} \cdot \vec{S} + hc \vec{S} \cdot \vec{A} \cdot \vec{I}$$

where all the symbols have their usual meanings.^{14b} Provision was

made for two of the principal axes in one plane of the \vec{g} and nuclear hyperfine, \vec{A} , tensors to be noncoincident. Here the molecular-axis system is designated as X, Y, Z . The axis systems which diagonalize the \vec{g} and \vec{A} tensors are designated x, y, z and x', y', z' , respectively. α_{xz} is defined as the angle of noncoincidence in the XZ plane (angle between z and z' or x and x' with y and y' coaxial), and similarly α_{xy} is defined as the angle of noncoincidence in the XY plane (angle between x and x' or y and y' with z and z' coaxial). The simulated spectra were sums of spectra of randomly oriented complexes with $I = 5/2$ and $I = 0$ isotopes weighted according to their natural abundances.

g factors were obtained readily by computer fitting the $I = 0$ peaks in the calibrated X-band frozen-solution spectra. The anisotropy in the g factors was further refined by use of the corresponding Q-band

Table II. Visible Spectra Results^a

compd	λ_{\max} , nm	$10^{-3}\epsilon$, cm ⁻¹ M ⁻¹
(NH ₄) ₂ MoCl ₆ ^b	710	0.011
	445	0.010
I	528	4.00
	420	2.25
II (red)	520	1.92
	418	1.02
III (green)	~735 (broad)	~0.43
	~525 (shoulder)	
IV (trans?)	705	0.070
	472	0.638
V	645	0.650
VI	686	2.61
	532	3.71
	424	4.07
VII	433 (shoulder, well-defined)	7.29
VIII	526	2.65
	333	~2.5
	370 (shoulder)	
IX	510	~2.1
	355, 310 (shoulders)	
X	378	~0.012
	303	~0.016
	550, 460, 405, 360 (shoulders)	

^a In dimethylformamide solution. ^b In HCl solution; ref 2.

spectra. Preliminary A values were obtained directly from the frozen-solution spectra when possible. In most cases, only two of the principal A values could be measured, so the third was approximated by the relation A_0 (cm⁻¹) = ($A_{xx} + A_{yy} + A_{zz}$)/3, where A_0 was measured from the room-temperature solution spectrum.

About 20 simulation trials were required to achieve an optimum fit for compounds with coincident g - and A -tensor axes. When noncoincidence was present, approximately 30 trials were necessary. Rhombic-case simulations with coincident magnetic axes were based on nominally 8000 orientations of the complex relative to the applied magnetic field with a total of 500 field values at 2-G intervals. When g - and A -tensor axes were noncoincident, the number of orientations needed was doubled. Approximately 2.5 min of central processing unit time for the coincident-axes cases and 3–7 min for the noncoincident-axes cases were required. Inclusion of separate hyperfine coupling constants for the $I = 5/2$ isotopes (⁹⁵Mo and ⁹⁷Mo) in the calculations resulted in no appreciable improvement in fit.

Electronic Spectra. Solutions of the complexes (1×10^{-4} – 1×10^{-3} M) in deaerated DMF (spectral grade, dried over molecular sieves) were prepared and their electronic spectra recorded under dry N₂ by use of a Varian 635 recording spectrophotometer.

Results

Values of the magnetic parameters for the compounds studied are listed in Table I. The designations "cis" and

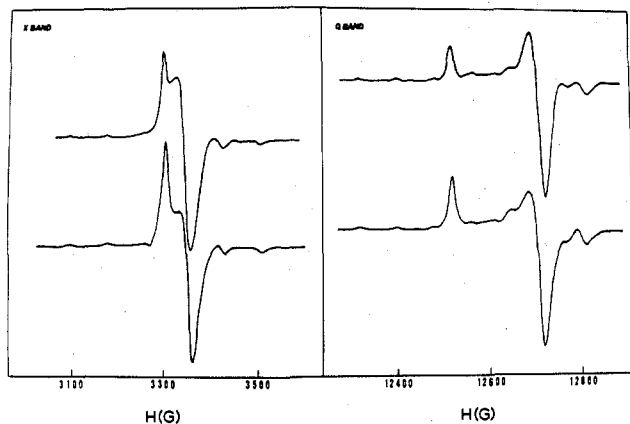


Figure 1. Experimental (upper) and simulated (lower) frozen-solution EPR spectra of $(\text{NH}_4)_2\text{MoOCl}_5$ at X-band (9.1 GHz) and Q-band (35 GHz) frequencies: example of an "axial" spectrum. Concentration is 2×10^{-3} M in dimethylformamide. Instrument settings: X-band modulation amplitude 5 G, scan rate 1000 G/16 min, power 10 mW, time constant 0.03 s, temperature 77 K; Q-band modulation amplitude 1 G, scan rate 1000 G/16 min, power 0.8 mW, temperature 110 K.

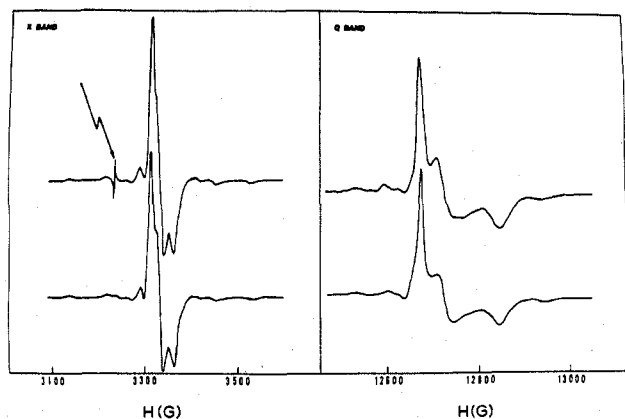


Figure 2. Experimental (upper) and simulated (lower) frozen-solution EPR spectra of *trans*- $\text{MoOCl}((\text{sal})_2\text{phen})$ at X-band and Q-band frequencies: example of a "rhombic" spectrum. EPR parameters are as in Table I. Other conditions are as in Figure 1. Arrow denotes resonance of DPPH.

"trans" refer to coordination of a chloro ligand relative to oxo. The results of the visible electronic spectra are given in Table II. Representative EPR spectra at both Q- and X-band frequencies and their respective computer simulations are reproduced in Figures 1–3. Figure 1 is an example of a compound, $(\text{NH}_4)_2\text{MoOCl}_5$, with axial symmetry, i.e., $g_{xx} = g_{yy} \neq g_{zz}$ and $A_{xx} = A_{yy} \neq A_{zz}$. The spectra of a complex, *trans*- $\text{MoOCl}((\text{sal})_2\text{phen})$, with rhombic symmetry ($g_{xx} \neq g_{yy} \neq g_{zz}$ and $A_{xx} \neq A_{yy} \neq A_{zz}$) and coincident *g*- and *A*-tensor axes are shown in Figure 2. Figure 3 is an example of a case, *cis*-(Et_4N) $\text{MoOCl}(\text{sap})$, in which the *g* and *A* tensors are both rhombic and noncoincident in the *XY* plane. Simulations with and without inclusion of noncoincidence are shown.

Discussion

Although EPR spectra of $(\text{NH}_4)_2\text{MoOCl}_5$ have been studied in a variety of media,^{15–21} the experiments have been repeated with DMF as the solvent in order to test our simulation procedure. Mabbs et al.¹⁹ found that at low concentration in DMF, MoOCl_5^{2-} dissociates a Cl almost completely at the axial position and that a molecule of DMF coordinates to form the complex $[\text{MoOCl}_4(\text{DMF})]^-$ ($g_0 = 1.947$). Even when Cl⁻ was added in a 60-fold excess with respect to $[\text{MoOCl}_4(\text{DMF})]^-$, MoOCl_5^{2-} ($g_0 = 1.940$)¹⁷ was still not detected. In fact, the spectrum¹⁴ attributed to MoOCl_5^{2-} in concentrated HCl is now believed¹⁷ to be that of $\text{MoOCl}_4\text{OH}_2^-$. Our

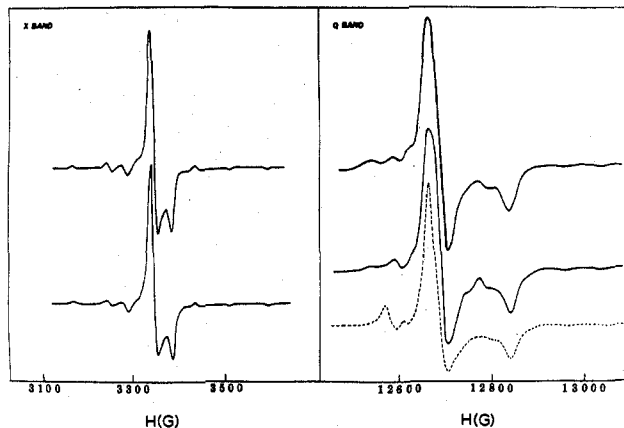


Figure 3. Experimental (upper) and simulated (lower) frozen-solution EPR spectra of *cis*-(Et_4N) $\text{MoOCl}_2(\text{sap})$ at X-band and Q-band frequencies: example of a "rhombic" spectrum with noncoincident principal axes of the *g* and nuclear hyperfine tensors in the *XZ* plane. The dashed curve in the Q-band spectrum shows the simulated EPR spectrum without inclusion of noncoincidence. EPR parameters are as in Table I. Other conditions are as in Figure 1.

room-temperature EPR spectrum of $(\text{NH}_4)_2\text{MoOCl}_5$ dissolved in DMF ($g_0 = 1.947$, $A_0 = 46.6 \times 10^{-4}$ cm⁻¹) is virtually identical with that of Mabbs and co-workers,¹⁹ so we assume that the species we are observing is $[\text{MoOCl}_4(\text{DMF})]^-$. Work on NO_3^- reduction by MoOCl_5^{2-} also indicates that the predominating species in DMF solution is $\text{MoOCl}_4(\text{DMF})^-$.²² The isotropic parameters calculated from the anisotropic parameters obtained from the frozen-solution EPR spectra are slightly different ($g_0(\text{calcd}) = 1.949$, $A_0(\text{calcd}) = 47.2 \times 10^{-4}$ cm⁻¹). An axial-spin Hamiltonian¹⁶ was used in our attempts to simulate the frozen-solution spectra. Since the g_{\perp} (high-field) region of the spectra could not be fit exactly with this Hamiltonian (Figure 1), it is possible that a slight rhombic distortion of the complex is introduced by the coordination of DMF.

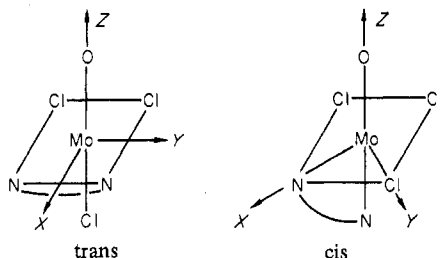
A problem arises also in the interpretation of visible electronic spectra of $4d^1$ MoO^{3+} complexes. Gray and Hare²³ observed the spectrum of what was believed to be MoOCl_5^{2-} in 12 M HCl. This complex belongs to the point group C_{4v} , and if the *X* and *Y* axes are defined to be along the equatorial Mo–Cl bonds, the ground state will be predominantly $|XY\rangle$ (b_2^*) in character. The lowest energy band in the spectrum, observed at 14050 cm⁻¹, was assigned to the $|XY\rangle$ (b_2^*) \rightarrow $|XZ\rangle$, $|YZ\rangle$ (e^*) transition and the band at 22500 cm⁻¹ to $|XY\rangle$ (b_2^*) \rightarrow $|X^2 - Y^2\rangle$ (b_1^*). The latter assignment has been questioned by Mabbs et al.,^{17,18} who as a result of polarization studies suggest that the band is due to an oxygen ($p\pi$) to metal ($3Z^2 - R^2$) or $|XY\rangle$ charge-transfer transition, ${}^2B_2 \rightarrow {}^2E$ in C_{4v} . It is generally accepted that the lowest energy band corresponds to the $b_2^* \rightarrow e^*$ transition, but beyond this no definite assignments have been made. The forbidden $b_2^* \rightarrow b_1^*$ transition is expected to be of low intensity and to be obscured by electronically allowed d–d transitions.

The large intensities of the bands for all the compounds in Table II except $(\text{NH}_4)_2\text{MoOCl}_5$ and IV ($\text{MoOCl}(\text{acac})_2$) and the lack of correlation of the reciprocal of the energy of the longest wavelength bands with $g_{\perp} = (g_{xx} + g_{yy})/2$ values indicate that these transitions are not of d–d origin. This is unfortunate since the amount of structural information obtainable from the EPR data reported here is consequently limited.

Compounds I–X possess at most C_{2v} symmetry, so the *g*-factor equations given by Manoharan and Rogers¹⁶ and by DeArmond et al.²⁰ are inappropriate. Not only must the difference in energy between the $|XZ\rangle$ and $|YZ\rangle$ orbitals caused by the lower symmetry ligand field be included but also,

in complexes with symmetries of C_{2v} or lower, the possibility of configurational mixing of d orbitals belonging to the same irreducible representation as the ground state must be taken into account.^{24,25} Due to the wide disparity in the ligands in the XY planes of the compounds being discussed here, it is difficult to make comparisons of the EPR parameters among the entire group. For this reason, the remainder of the discussion will be focused mainly upon the individual complexes and upon attempts to correlate the EPR results with their structures.

trans-MoOCl₃(phen) (I) and trans-MoOCl₃(bpy) (II). Both compounds I and II are likely trans isomers as they exhibit very similar EPR and optical spectral properties (Tables I and II) which are quite different from those of *cis*-MoOCl₃(bpy), whose structure is known from X-ray crystallography.^{11a} Both isomers possess a mirror plane, σ_{XZ} , and hence belong to the point group $C_s^{(XZ)}$.



It is not possible to distinguish isomers in this instance by noncoincident **A**- and **g**-tensor axes since noncoincident axes are possible in the XZ plane in both cases and are in fact observed experimentally (Table I). Nor is it possible to use the EPR parameters of these complexes to unequivocally assign geometries. Unexpectedly, the values of g_0 , A_0 , g_{\perp} , g_{zz} , and A_{\perp} [$A_{\perp} = (A_{xx} + A_{yy})/2$] for compounds I and II are nearly identical with those of $(NH_4)_2MoOCl_5$. Moreover, g_{zz} with its origin presumably in metal and chlorine spin-orbit coupling¹⁶ should reflect the ligand field equatorial to the MoO bond axis. However, comparison of values for $(NH_4)_2MoOCl_5$ and the trans and cis compounds II and III shows no obvious trends. A number of effects appear to be operating here. It is possible contributions to the g shift of Mo(V) complexes arise from low-energy charge-transfer transitions of appropriate symmetry in addition to the ligand field bands.¹⁹

Information about the orientation of the principal axes of the **g** and **A** tensors relative to the molecular axis system is not normally obtainable from EPR spectra of frozen solutions. Here, however, the observed noncoincidence for compounds I–III defines the XZ plane. Symmetry requires that the directions of g_{yy} and A_{yy} be coaxial and normal to this plane. A_{xx} and A_{zz} (the largest hyperfine splitting) are expected to lie nearly along the molecular X and Z (MoO³⁺ bond) axes, respectively, since these tensor components are largely governed by the ground-state antibonding metal-based molecular orbital, consisting primarily of $|XY\rangle$ (cis) or $|X^2 - Y^2\rangle$ (trans), in which the unpaired electron resides.²⁴ This has been found to be the case in a single-crystal study of $MoOCl_3[P(NMe_2)O]_2$ which also has C_s symmetry and noncoincident tensor axes with $\alpha_{XZ} = 22^\circ$.²⁵ We assign g_{zz} to be that component of the **g** tensor which has its direction closest to that of A_{zz} .

For the trans compounds I and II, the $|XZ\rangle$, $|3Z^2 - R^2\rangle$, and $|X^2 - Y^2\rangle$ metal orbitals transform as A' and the $|XY\rangle$ and $|YZ\rangle$ orbitals as A'' in $C_s^{(XZ)}$. Since the X and Y axes are oriented between the bonds, the ground-state molecular orbital will be predominantly $|X^2 - Y^2\rangle$ in character. An admixture of some $|3Z^2 - R^2\rangle$ character into the ground state will result in a rhombic distortion; i.e., the lobes along the X and Y axes will no longer be equal in size.²⁴ On the other hand, a small mixing of some $|XZ\rangle$ into the ground state will result

in a slight rotation of the ground-state orbital out of the XY plane about the Y axis. If we write a wave function for the new ground-state metal orbital taking these effects into account, it will be of the form

$$\psi_{X^2-Y^2}^{a''} = a_1|X^2 - Y^2\rangle + b_1|XZ\rangle + c_1|3Z^2 - R^2\rangle$$

where we can assume that $a_1 \gg b_1, c_1$ since the $|XZ\rangle$ and $|3Z^2 - R^2\rangle$ orbitals will likely be high in energy. This type of mixing may also result in a small deviation of the A_{zz} direction from the molecular z axis. The other metal-based antibonding wave functions, not in order of increasing energy, can also be written

$$\psi_{XZ}^{a''} = a_2|XZ\rangle + b_2|X^2 - Y^2\rangle + c_2|3Z^2 - R^2\rangle$$

$$\psi_{3Z^2-R^2}^{a''} = a_3|3Z^2 - R^2\rangle + b_3|X^2 - Y^2\rangle + c_3|XZ\rangle$$

$$\psi_{XY}^{a''} = a_4|XY\rangle + b_4|YZ\rangle$$

$$\psi_{YZ}^{a''} = a_5|YZ\rangle + b_5|XY\rangle$$

where normalization conditions require $a_4 = \cos \alpha_{XZ}$, $b_4 = \sin \alpha_{XZ}$, $a_5 = \cos \alpha_{XZ}$, and $b_5 = \sin \alpha_{XZ}$.

The intermixing of the metal orbitals of A'' symmetry results in a rotation about the Y axis of the $\psi_{XY}^{a''}$, $\psi_{YZ}^{a''}$ pair as a unit, the angle of rotation α_{XZ} being dependent upon the degree of mixing. The origin of the noncoincidence of **g**- and **A**-tensor axes in the XZ plane can be seen clearly. Since the directions of g_{xx} and g_{zz} will be approximately orthogonal to the planes of the $\psi_{YZ}^{a''}$ and $\psi_{XY}^{a''}$ orbitals, respectively,^{23,26} these axes will be rotated away from the X and Z axes, along which the principal **A**-tensor axes are assumed to lie.²⁴ Moreover, since the angles of rotation are quite large, 25–35°, the energies of the $|XY\rangle$ and $|YZ\rangle$ orbitals must be reasonably close to accommodate such extensive mixing.

It is also possible to take covalency into account by including linear combinations of ligand orbitals of the appropriate symmetries to form expressions for molecular orbital wave functions. Due to the complexity of the problem, a qualitative approach will be taken both in predicting the effects of orbital mixing due to the low-symmetry ligand field and in predicting the relative energies of $\psi_{YZ}^{a''}$ and $\psi_{XZ}^{a''}$ with respect to the ground state. We will refer to these energies as ΔE_{YZ} and ΔE_{XZ} upon which g_{xx} and g_{yy} partly depend, respectively.²⁷

By use of simple crystal field arguments, we predict for *trans*-MoOCl₃(phen) that $\Delta E_{XZ} > \Delta E_{YZ}$ and therefore $g_{yy} > g_{xx}$. However, Hitchman et al.^{24,28} predict that when the asymmetric component of the ligand field (in this case along the X axis) lies along the ground-state orbital lobe directions, the g_{xx} , g_{yy} anisotropy is due predominantly to the mixing of $|3Z^2 - R^2\rangle$ into the ground state rather than to the ΔE_{XZ} , ΔE_{YZ} difference. Depending upon the sign of the mixing coefficient c_1 , the anisotropy in g_{xx} and g_{yy} caused by the ΔE_{XZ} , ΔE_{YZ} difference can be either augmented or canceled.^{24,26} Since we observe g_{xx} slightly greater than g_{yy} , it appears that the $|3Z^2 - R^2\rangle$ mixing mechanism with a negative c_1 does predominate here.

cis-MoOCl₃(bpy) (III). In the cis compound III, the axes point along the equatorial metal–ligand bonds rather than between them. The ground state in $C_s^{(XZ)}$ is therefore predominantly $|XY\rangle$ (A''):

$$\psi_{XY}^{a''} = a_1|XY\rangle + b_1|YZ\rangle$$

Expressions for the excited-state metal d-orbital combinations can be written as

$$\psi_{YZ}^{a''} = a_2|YZ\rangle + b_2|XY\rangle$$

$$\psi_{X^2-Y^2}^{a''} = a_3|X^2 - Y^2\rangle + b_3|XZ\rangle + c_3|3Z^2 - R^2\rangle$$

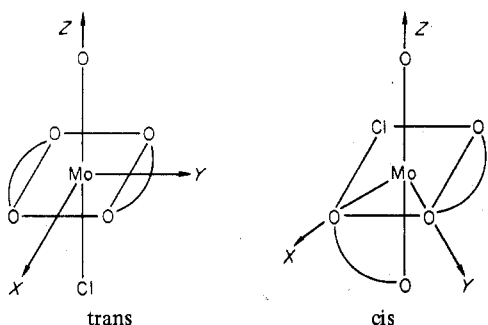
$$\psi_{XZ}^{a''} = a_4|XZ\rangle + b_4|X^2 - Y^2\rangle + c_4|3Z^2 - R^2\rangle$$

$$\psi_{3Z^2-R^2}^{a''} = a_5|3Z^2 - R^2\rangle + b_5|X^2 - Y^2\rangle + c_5|XZ\rangle$$

A mixing of some $|YZ\rangle$ character into the ground state will have the effect of tilting the ground-state orbital out of the XY plane about the Y axis. Since mixing of $|3Z^2 - R^2\rangle$ into the ground state is not permitted by the symmetry in this case, any g_{xx} , g_{yy} anisotropy should be largely due to the ΔE_{XZ} , ΔE_{YZ} difference. If it is assumed that the presence of the bipyridyl bridge and of N ligand along the X axis will cause ψ_{XZ}^{a*} to be higher in energy than ψ_{YZ}^{a*} , it would be expected that $g_{xx} > g_{yy}$ as observed experimentally (Table I). It would also be expected that the g_{xx} and g_{zz} directions will be dependent upon the spatial orientations of the ψ_{XZ}^{a*} and $\psi_{X^2-Y^2}^{a*}$ orbitals, respectively.²⁷

It is also found here that $g_{zz} < g_{xx}$, g_{yy} , which might not be expected¹³ for a complex with three equatorial Cl ligands, if chlorine ligand spin-orbit coupling is the cause of the unusually high values of g_{zz} in $(\text{NH}_4)_2\text{MoOCl}_5$.¹⁶

trans-MoOCl(acac)₂ (IV). MoOCl(acac)₂ could be either cis or trans.



The trans structure belongs to the point group C_{2v} , which requires that all tensor axes be coincident. This is what is observed experimentally (Table I). In all the cis compounds reported here, noncoincidence is observed in at least one principal plane (Table I). However, the lack of observed noncoincident axes for compound IV in itself does not preclude the cis structure (which has no symmetry and therefore places no restrictions on the directions of the principal axes). It is possible that the angles of noncoincidence could be too small ($<5^\circ$) to be observed experimentally. Other data discussed below, however, provide further evidence for a trans structure. It is noteworthy that in the limited number of compounds (III, VI, and X) whose X-ray structures have been determined¹¹ the cis isomer has been found.

Changes in the visible spectrum in DMF upon standing have been observed for MoOCl(acac)₂, suggesting dissociation of Cl⁻ and possible formation of the cis isomer. This is expected to be more likely for a more labile trans chloro ligand than for cis, in agreement with the EPR results. Also, the reduction of NO_3^- by this complex is very slow, again suggesting a trans complex.⁶

Since all four equatorial ligands are oxygen atoms in the trans structure, the A-tensor anisotropy in the XY plane is expected to be small, as is experimentally observed. In this case the equations given by Manoharan and Rogers¹⁶ for the g and A values are applicable to a first approximation. The value of β_2^* , the coefficient of the metal part of the in-plane π -bonding molecular orbital is calculated to be 0.98. This result indicates that the amount of in plane π bonding is very small, which is to be expected since the oxygen ligands in the trans structure do not have orbitals available for π bonding in the XY plane but do in the cis structure. As a result of the calculation above, an average value for ϵ , the coefficient for the metal part of the out-of-plane π -bonding molecular orbital, is obtained. In this case it is found that $\epsilon = 0.80$, which is indicative of quite strong out-of-plane π bonding, again consistent with a trans structure. This is apparently the result of the proximity of the full p_z orbitals on the oxygen atoms

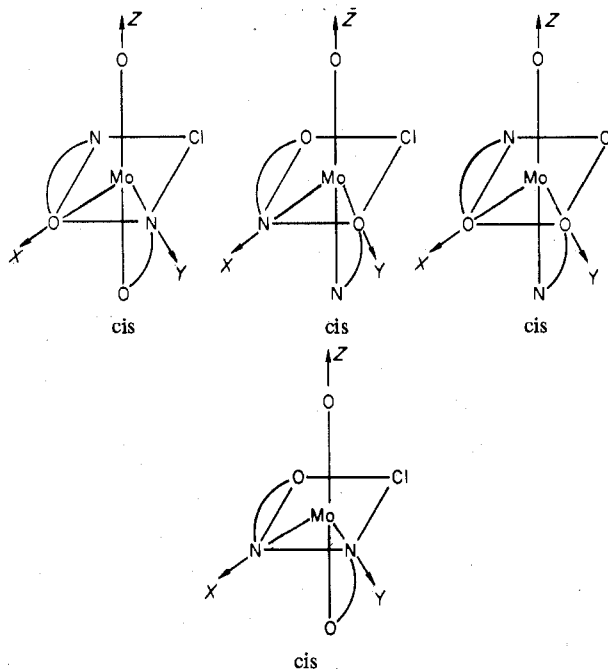
to the empty $|XZ\rangle$ and $|YZ\rangle$ orbitals on the metal.

In C_{2v} , there is the possibility of mixing $|3Z^2 - R^2\rangle$ into the predominantly $|X^2 - Y^2\rangle$ ground state, since both $|3Z^2 - R^2\rangle$ and $|X^2 - Y^2\rangle$ transform as A_1 . Again the asymmetric component of the ligand field in the XY plane lies along the ground-state orbital directions, so the g_{xx} , g_{yy} anisotropy should be due primarily to the $|3Z^2 - R^2\rangle$ mixing.^{24,28} If the ground-state metal orbital is written

$$\psi_{X^2-Y^2}^{a*} = a|X^2 - Y^2\rangle + b|3Z^2 - R^2\rangle$$

we would expect $b < 0$ in this case,^{24,27} and consequently we tentatively assign $g_{xx} > g_{yy}$ in Table I.

cis-MoOCl(ox)₂ (V). The EPR results for MoOCl(ox)₂ have been discussed previously by Spence et al.⁶ in relationship to the kinetics of nitrate reduction. Since none of the principal axes of the g and A tensors are coincident, the complex must not possess symmetry. Only a cis structure is consistent with this observation. There are four possible cis isomers, viz.

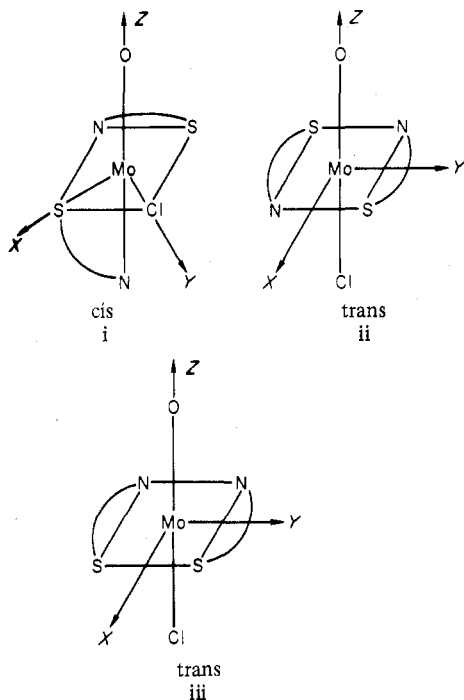


The EPR results do not readily distinguish between these isomers.

cis-MoOCl(tox)₂ (VI). The structure of cis-MoOCl(tox)₂ has been shown by X-ray crystallography to be i in the solid state.^{11b} We find that complex i doped into the isostructural diamagnetic host lattice MoO₂(tox)₂ has principal g factors identical with those of the complex dissolved in DMF, thus confirming that the solid-state and solution structures both correspond to i.

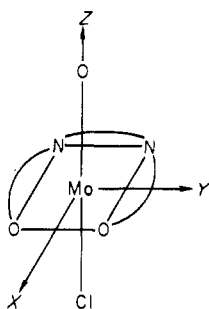
The noncoincidence data, $\alpha_{xy} = 10^\circ$ (Table I), are consistent with either structure i or ii. In cis structure i none of the principal tensor components need be coincident although experimentally g_{zz} and $A_{z'z'}$ appear to be coaxial or nearly so. The C_2 axis of structure ii requires that g_{zz} and $A_{z'z'}$ be coincident but places no restriction on the tensor components in the XY plane. The EPR data preclude trans structure iii since the mirror plane requires that g_{yy} and $A_{y'y'}$ be coincident and perpendicular to it. Because of the largely $|XY\rangle$ ground state, the largest hyperfine splitting $A_{z'z'}$ (and approximately coaxial g_{zz}) must correspond to the Mo-O bond axis.

The similarities in the EPR parameters (Table I) for VI, cis-MoOCl(tox)₂, VIII, cis-MoOCl(C₈H₁₈N₂S₂), and IX, cis-MoOCl(C₁₀H₂₂N₂S₂), suggest similar structures. The unusually large value of $g_{zz} = 2.003$ is consistent with the results of previous work on MoO³⁺ complexes with sulfur ligands.^{3,4,7}



The EPR parameters reported here for dissolved crystalline $\text{MoOCl}(\text{tox})_2$ are quite different from those of Marov et al. ($g_0 = 1.9805$, $A_0 = 31.8 \times 10^{-4} \text{ cm}^{-1}$),^{29a} who prepared the complex in situ. Several species which depend on the Cl^-/tox ratio are known to exist in solution.^{29b}

trans- $\text{MoOCl}(\text{sal})_2(\text{phen})$ (VII). No X-ray crystallographic data are yet available for this compound, but because of the rigid structure of the $((\text{sal})_2\text{phen})$ ligand it is quite certain that the chelate is planar and that the chloride is coordinated in the axial position, viz.



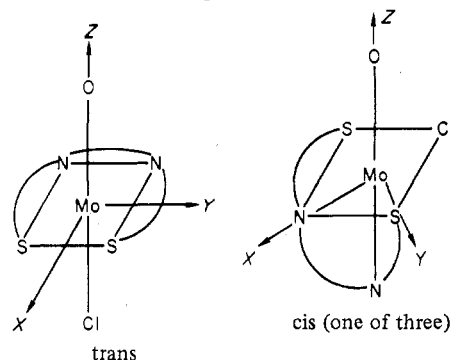
Because of the presence of σ_{XZ} , noncoincidence may occur in only the XZ plane. However, the EPR spectra could be fit satisfactorily with all magnetic axes coincident.

Room-temperature EPR spectra of $\text{MoOCl}((\text{sal})_2\text{phen})$ in DMF or dichloromethane (not specified) have been obtained by Dilworth and co-workers ($g_0 = 1.938$, $A_0 = 42 \times 10^{-4} \text{ cm}^{-1}$).³⁰ Our results differed slightly from theirs. At first it appeared that the spectra were of two fairly distinct species with similar g and A values, possibly a mixture of $\text{MoOCl}((\text{sal})_2\text{phen})$ and $[\text{MoO}((\text{sal})_2\text{phen})\text{DMF}]^+$. Upon addition of an excess of Et_4NCl to the solution, the spectrum became one of a single species ($g_0 = 1.940$, $A_0 = 44 \times 10^{-4} \text{ cm}^{-1}$), presumably $\text{MoOCl}((\text{sal})_2\text{phen})$. It appears that the previous workers observed either the DMF complex or an unresolved mixture of the two.

As in the case of I, *trans*- $\text{MoOCl}_3(\text{bpy})$, and II, *trans*- $\text{MoOCl}_3(\text{phen})$, g -tensor anisotropy in the XY plane can arise both from the difference in ΔE_{XZ} and ΔE_{YZ} and from a mixing of $|3Z^2 - R^2\rangle$ into the ground state $|X^2 - Y^2\rangle$ orbital. Because of intraligand π bonding in the N-O bridging groups, one anticipates that ΔE_{YZ} will be greater than ΔE_{XZ} and therefore

$g_{xx} > g_{yy}$.²⁴ Crystal field arguments favor a negative c_1 coefficient in $C_5^{(XZ)}$ symmetry causing contraction of the negative lobe of the ground state along the Y axis to avoid the effect of the nitrogen-oxygen bridges. This mechanism also leads to $g_{xx} > g_{yy}$. We therefore tentatively assign the larger g_{\perp} value in Table II to g_{xx} .

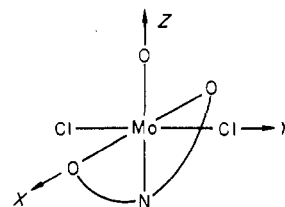
cis- $\text{MoOCl}(\text{C}_8\text{H}_{18}\text{N}_2\text{S}_2)$ (VIII). Preliminary EPR results have been reported for this compound.⁷ Its frozen-solution EPR spectra at both X and Q band are nearly superimposable upon those of *cis*- $\text{MoOCl}(\text{tox})_2$. There are four possible structures for $\text{MoOCl}(\text{C}_8\text{H}_{18}\text{N}_2\text{S}_2)$, one *trans* and three *cis*: one with a nitrogen in the axial position and *cis* sulfurs, another with nitrogen axial but with *trans* sulfurs, and a third with a sulfur atom in the axial position.



There is noncoincidence in the XY plane and possibly a small angle of noncoincidence, $\sim 5-10^\circ$, between g_{zz} and $A_{z'z'}$. By following similar arguments used earlier, we conclude that the compound is *cis*. The similarity between the EPR spectra of compounds VI and VIII suggests that the *cis* structure is probably that shown here with the sulfur atoms *cis* to the oxo atom but *trans* to one another. In addition, the low values of A_0 and $A_{z'z'}$ and the high values for g_{zz} and g_0 suggest two sulfur atoms *cis* to the oxo.^{3,4,7} The slightly greater rhombicity in the XY plane for compound VIII compared with that for compound VI could be due to differences in bridging ligands for the two compounds.

cis- $\text{MoOCl}(\text{C}_{10}\text{H}_{22}\text{N}_2\text{S}_2)$ (IX). The $\text{C}_{10}\text{H}_{22}\text{N}_2\text{S}_2$ ligand⁸ is very similar in structure to $\text{C}_8\text{H}_{18}\text{N}_2\text{S}_2$, so the discussion is parallel. Again the EPR data indicate a *cis* ligand arrangement. The rhombic g values and large g_0 and g_{zz} and low A_0 and $A_{z'z'}$ values indicate that there are probably two equatorial sulfur atoms.^{3,4,7} The larger g -tensor anisotropy in the XY plane observed for $\text{MoOCl}(\text{C}_{10}\text{H}_{22}\text{N}_2\text{S}_2)$ (0.015) as compared to that for $\text{MoOCl}(\text{C}_8\text{H}_{18}\text{N}_2\text{S}_2)$ (0.009) could reflect ligand-bridging effects or possibly *cis* arrangement on the sulfurs in the former compound and a *trans* arrangement in the latter.

cis- $\text{Et}_4\text{NM}(\text{OCl})_2(\text{sap})$ (X). The structure of this complex has been shown to be *cis*



by X-ray crystallography.^{11a} Due to the asymmetry of the *sap* ligand, the complex has at most $C_5^{(XZ)}$ symmetry. It is therefore possible to observe noncoincidence of g - and A -tensor axes at least in the XZ plane. In fact a noncoincidence of about $\alpha_{XZ} = 20^\circ$ is observed. The unpaired electron in this case would be expected to be found in an orbital consisting mainly of $|XY\rangle$. As in the case of *cis*- $\text{MoOCl}_3(\text{bpy})$, mixing of $|3Z^2 - R^2\rangle$ into the ground state is not possible, so the g_{xx} ,

g_{yy} anisotropy must be due primarily to the ΔE_{XZ} , ΔE_{YZ} difference. We find that $A_{zz} > A_{xx}$, A_{yy} as would be expected,¹⁶ but $g_{zz} < g_{xx}$, g_{yy} even though there are two Cl ligands present in equatorial positions, which should raise g_{zz} if the chloride ligand spin-orbit coupling mechanism is operating.¹⁶

Xanthine Oxidase (XI). The "very rapid" signal of xanthine oxidase is characterized by the parameters³ $g_1 = 2.025$, $g_2 = 1.956$, $g_3 = 1.951$; $A_1 = 38 \times 10^{-4} \text{ cm}^{-1}$, $A_2 = 21 \times 10^{-4} \text{ cm}^{-1}$, $A_3 = 35 \times 10^{-4} \text{ cm}^{-1}$. The large value of g_1 has been taken as evidence for sulfur ligation.³ We note that in all the molybdenyl complexes examined here the most extreme g value (g_{zz}) is always associated with the largest hyperfine splitting, A_{zz} , which is much greater than A_{xx} and A_{yy} . However, in the case of the enzyme this is not so. This suggests that the ground-state orbital of the enzyme is different from those of the model complexes ($|XY\rangle$ or $|X^2 - Y^2\rangle$), with Z along MoO^{3+} . Such might be the case if the Mo(V) species of the enzyme is not MoO^{3+} . Recent EPR results by Bray et al. suggest a terminal MoS group may be present in the oxidized enzyme (Mo(VI) state). Upon reduction, the MoS group is protonated to MoSH, giving rise to the observed proton superhyperfine splitting.³³ Further studies are needed on low-symmetry Mo^{5+} and MoO^{3+} complexes employing magnetically dilute single crystals to determine the orientation of g - and A -tensor axes relative to the bond directions before more definitive conclusions can be drawn.

Summary and Conclusions

Several of the compounds studied here exhibit rather large angles of noncoincidence of principal components of the g and hyperfine tensors (Table I). The large angles of rotation can be explained by a model in which extensive mixing among excited-state d orbitals takes place, although ligand spin-orbit coupling could contribute to the observed rotation as well.³¹ Single-crystal studies are needed to better delineate these effects. The observation of noncoincident tensor components has been shown to be of use in precluding certain geometrical isomers in solution.

No correlation exists between the magnitude of g_{zz} and the number of equatorially coordinating Cl^- ions. Therefore, it seems doubtful that chlorine spin-orbit coupling is the dominant g -shift mechanism for the complexes with $g_{zz} > g_{\perp}$. Charge-transfer states of appropriate symmetry may be important. Most of the compounds show relatively low-energy bands of high intensity which are likely charge transfer in origin. The in-plane g_{xx} , g_{yy} anisotropy is explicable in terms of a difference in ΔE_{XZ} and ΔE_{YZ} and/or mixing of $|3Z^2 - R^2\rangle$ into the ground-state orbital.

The well-known inverse correlation of A_0 with g_0 ³² is followed by the compounds in Table I; however, the points do not cluster in domains according to the identity of equatorial ligand donor atoms. In contrast, clustering has been found for VO^{2+} complexes and has aided in assigning the coordinating ligands.¹⁴ In the case of MoO^{3+} complexes with equatorial sulfur ligands, one invariably finds low values of A_0 with $g_{zz} > 2.0$.

Acknowledgment. This work was supported by Grants GM-08437 and GM-20194 from the National Institutes of Health and by the AMAX Foundation, Inc., to which thanks

are gratefully expressed. The authors wish to thank Mr. G. Daniel Templeton for assistance with the computer simulations.

Note Added in Proof. Further refinement of the crystal structure of $\text{X}((\text{Et}_4\text{N})\text{MoOCl}_2(\text{sap}))$ ^{11b} reveals that the axial N ligand is displaced from the molybdenyl Mo-O bond direction by $\sim 8^\circ$ in the XZ plane in accordance with the noncoincidence of the g - and A -tensor axes observed in the EPR spectra of this complex.

Registry No. I, 38237-92-2; II, 35408-53-8; III, 35408-54-9; IV, 17871-02-2; V, 30052-13-2; VI, 67650-71-9; VII, 64085-34-3; VIII, 71301-37-6; IX, 71328-31-9; X, 71264-61-4; $(\text{NH}_4)_2\text{MoOCl}_5$, 17927-44-5.

References and Notes

- (1) (a) University of New Hampshire. (b) Utah State University. (c) University of Arizona.
- (2) E. I. Stiefel, *Prog. Inorg. Chem.*, **22**, 1 (1977).
- (3) R. C. Bray, *Enzymes*, 3rd Ed., **12**, 299 (1975).
- (4) R. C. Bray and T. Vanngard, *Biochem. J.*, **114**, 725 (1969).
- (5) R. C. Bray, T. Vanngard, and L. S. Merriwether, *Nature (London)*, **212**, 467 (1966).
- (6) R. D. Taylor, P. G. Todd, N. D. Chasteen, and J. T. Spence, *Inorg. Chem.*, **18**, 44 (1979).
- (7) J. T. Spence, M. Minelli, P. Kroneck, M. I. Scullane, and N. D. Chasteen, *J. Am. Chem. Soc.*, **100**, 8002 (1978).
- (8) Abbreviations used: (I) phen = *o*-phenanthroline; (II, III) bpy = α, α' -bipyridyl; (IV) acac = acetylacetonate; (V) ox = 8-hydroxyquinoline; (VI) tox = 8-mercaptoquinoline; (VII) (sal)₂phen = disalicylaldehyde *o*-phenylenediamine; (VIII) $\text{C}_6\text{H}_{16}\text{N}_2\text{S}_2 = N, N'$ -dimethyl-*N, N'*-bis(2-mercaptoethyl)ethylenediamine; (IX) $\text{C}_{10}\text{H}_{22}\text{N}_2\text{S}_2 = N, N'$ -bis(2-methyl-2-mercaptoethyl)ethylenediamine; (X) sap = salicylaldehyde *o*-hydroxyanil.
- (9) H. K. Saha and M. C. Halder, *J. Inorg. Nucl. Chem.*, **33**, 3719 (1971); **34**, 3097 (1972).
- (10) R. L. Dutta and B. Chatterjee, *J. Indian Chem. Soc.*, **47**, 673 (1970).
- (11) (a) J. Enemark and K. Yamanouchi, unpublished data; (b) K. Yamanouchi and J. Enemark, *Inorg. Chem.*, in press.
- (12) W. G. Palmer, "Experimental Inorganic Chemistry", Cambridge University Press, Cambridge, England, 1934, p 408.
- (13) L. K. White and R. L. Belford, *J. Am. Chem. Soc.*, **98**, 4428 (1976).
- (14) (a) L. K. White, N. Albanese, and N. D. Chasteen, unpublished work; (b) L. K. White and N. D. Chasteen, *J. Phys. Chem.*, **83**, 279 (1979).
- (15) C. R. Hare, I. Bernal, and H. B. Gray, *Inorg. Chem.*, **1**, 831 (1962).
- (16) P. T. Manoharan and M. T. Rogers, *J. Chem. Phys.*, **49**, 5510 (1968).
- (17) C. D. Garner, L. H. Hill, F. E. Mabbs, D. L. McFadden, and A. T. McPhail, *J. Chem. Soc., Dalton Trans.*, 1299 (1975).
- (18) C. D. Garner, I. H. Hillier, J. Kendrick, and F. E. Mabbs, *Nature (London)*, **258**, 138 (1975).
- (19) C. D. Garner, M. R. Hyde, and F. E. Mabbs, *Inorg. Chem.*, **15**, 2327 (1976).
- (20) K. DeArmond, B. B. Garrett, and H. S. Gutowsky, *J. Chem. Phys.*, **42**, 1019 (1965).
- (21) H. Kon and N. E. Sharpless, *J. Phys. Chem.*, **70**, 105 (1966).
- (22) R. D. Taylor and J. T. Spence, *Inorg. Chem.*, **14**, 2815 (1975).
- (23) H. B. Gray and C. R. Hare, *Inorg. Chem.*, **1**, 363 (1962).
- (24) M. A. Hitchman, C. D. Olson, and R. L. Belford, *J. Chem. Phys.*, **50**, 1195 (1969).
- (25) G. D. Garner, P. Lambert, F. E. Mabbs, and T. J. King, *J. Chem. Soc., Dalton Trans.*, 1191 (1977).
- (26) α_{XZ} in the equation for the coefficients is the angle of noncoincidence provided that the ground state is pure $|X^2 - Y^2\rangle$, i.e., mixing is not significant.
- (27) B. R. McGarvey, *Transition Met. Chem.*, **3**, 160 (1966).
- (28) M. A. Hitchman and R. L. Belford, *Inorg. Chem.*, **8**, 958 (1969).
- (29) (a) I. N. Marov, V. K. Belyaeva, Y. N. Vubrov, and A. N. Ermakov, *Russ. J. Inorg. Chem. (Engl. Transl.)*, **17**, 515 (1972); (b) I. N. Marov, E. M. Reznik, V. K. Belyaeva, and Y. N. Dubrov, *ibid.*, **17**, 700 (1972).
- (30) J. R. Dilworth, C. A. McAuliffe, and B. J. Sayle, *J. Chem. Soc., Dalton Trans.*, 849 (1977).
- (31) C. P. Keijzers and E. DeBoer, *Mol. Phys.*, **29**, 1007 (1975).
- (32) B. A. Goodman and J. B. Raynor, *Adv. Inorg. Chem. Radiochem.*, **13**, 135 (1970).
- (33) S. Gutteridge, S. J. Tanner, and R. C. Bray, *Biochem. J.*, **175**, 887 (1978).